24

Morphology Control of Ordered Mesoporous Carbon Using Organic-Templating Approach

Shunsuke Tanaka[1] and Norikazu Nishiyama[2]
[1]*Department of Chemical, Energy and Environmental Engineering*
Faculty of Environmental and Urban Engineering, Kansai University
[2]*Division of Chemical Engineering*
Graduate School of Engineering Science, Osaka University
Japan

1. Introduction

The discovery of nanostructured carbon materials such as fullerenes (Kroto et al., 1985) and carbon nanotubes (Iijima, 1991) has led to a considerable interest in the development of various carbonaceous materials. In particular, porous carbonaceous materials have been attracting much attention because of their high surface area, large pore volume, chemical inertness, and high mechanical stability. Porous carbons show promise in the fields of hydrogen-storage, catalysis, separation, nanoreactors, electrochemistry, and biochemical engineering. Traditional synthesis methods, which involve carbonization of activated carbon (Marsh et al., 1971; Tamai et al., 1996; Hu et al., 2000), produce only disordered materials. To date, fabrication of highly ordered structure remains challenging. Research efforts to produce porous carbon materials with well-tailored pore systems have focused on the use of various inorganic template materials such as porous anodic aluminum oxide (AAO) films (Kyotani et al., 1995, 2006), zeolites (Kyotani et al., 1997; Ma et al., 2000; Nishihara et al., 2009), siliceous opals (Zakhidov et al., 1998; Yu et al., 2002), and mesoporous silicas (Ryoo et al., 1999; Lee et al., 1999; Kaneda et al., 2002; Kleitz et al., 2003; Xia et al., 2006) to template the carbon.

The use of zeolites, which have 3-dimensionaly connected framework structures constructed from corner-sharing TO_4 tetrahedra, where T is any tetrahedrally-coordinated cation such as Si and Al, as templates for the synthesis of carbon deposits on the micropore walls has been successful. The resulting materials have ordered and uniform angstrom-sized pores. However, long-range ordered microporous carbon replicas require repetitive carbonization steps to completely fill the template pores.

Silica opals, also called colloidal crystals, which are made by the self-assembly of uniform submicrometre-sized silica spheres, have been used as templates for the synthesis of ordered macroporous carbons. The porosity and contact sites between the silica spheres provided walls and interconnected spherical pores, respectively, in the resulting carbons.

Similarly, synthesis of ordered mesoporous carbons has focused on the use of ordered mesoporous silicas with interconnected pore structures as templates. Ordered structures of mesoporous silicas are derived from the self-assembly of surfactants and silica precursors.

The development of the M41S family (Kresge et al., 1992; Beck et al., 1992; Zhao et al., 1998) triggered the synthesis of a wide variety of mesoporous materials with diverse symmetries using various surfactants. As a result, various mesoporous carbon nanostructures with different pore systems have been synthesized using a variety of different mesoporous silica templates (Fig. 1). Pore size is controllable by selecting silica templates of different lengths and adjusting the silica wall thickness, though there is no report of tailoring only the silica wall thickness of the mesoporous silicas with constant pore diameter.

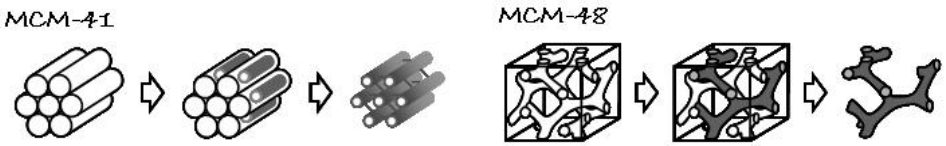

Fig. 1. Schematic illustration of the concept of M41S-template synthesis for ordered mesoporous carbons.

All the above inorganic-templating techniques require (1) preparation of inorganic templates, (2) impregnation of template pores with appropriate carbon precursors, (3) carbonization, and (4) subsequent selective removal of the templates using hydrofluoric acid or sodium hydroxide (Fig. 2). It is interesting to note that the pore system of carbons is inversely replicated from the silica templates, and thus, various mesostructured carbons with different pore systems have been synthesized using a variety of different mesoporous silica templates. Often, this time-consuming and costly process requires multiple infiltrations to complete the filling of the template pores. It is difficult to perform pore filling of the carbon precursors into the mesopores of silicas with low accessible pore systems.
Alternative methods, which eliminate the need for an inorganic template, have recently been developed to synthesize highly ordered mesoporous carbons, by directly assembly of organic templates with the carbon precursors (Tanaka et al., 2005, 2007, 2009; Meng et al., 2005; Zhang et al., 2005, 2006; Jin et al., 2009, 2010; Simanjuntak et al., 2009). This strategy uses an organic–organic interaction between a thermosetting resin and a thermally-decomposable copolymer to form a periodic ordered nanocomposite. The thermosetting

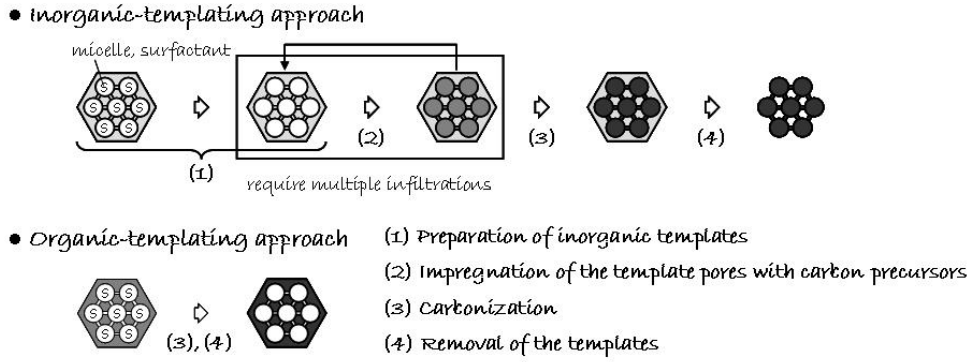

Fig. 2. Schematic illustration of the synthesis routes for ordered mesoporous carbons.

resin remains as the carbonaceous pore walls, while thermally-decomposable copolymer decomposes to form the mesopores (Fig. 2).
Simple techniques to control morphology and configuration of ordered mesoporous carbons are required for the development of practical applications. In this chapter, an advantageous organic-templating method for morphology control of ordered mesoporous carbons is introduced.

2. Self-assembly of organic–organic nanocomposites

In the inorganic-templating method, variable carbon precursors, e.g., sucrose, furfuryl alcohol, naphthalene, acetylene, polyacrylonitrile, and phenolic resin, can be utilized. On the other hand, in the organic-templating method, the main carbon precursors have been phenolic polymer resins prepared using phenolic resin monomer and formaldehyde (Fig. 3). The major reactions between phenolic resin monomer and formaldehyde include an addition reaction to form methylene and hydroxymethyl derivatives to form methylene and methylene ether bridged compounds. Interestingly, it has been pointed out that the polymerization mechanism and structure of resorcinol/formaldehyde are analogous to that described for the sol–gel processing of silica (Pekala 1989).

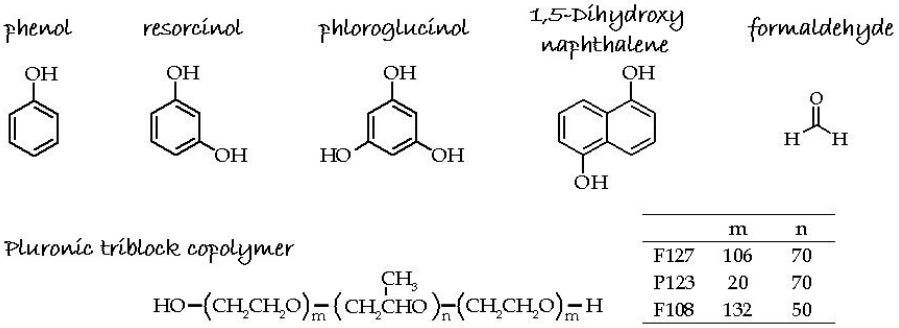

Fig. 3. Typical molecular structures of carbon precursors and thermally-decomposable polymer templates.

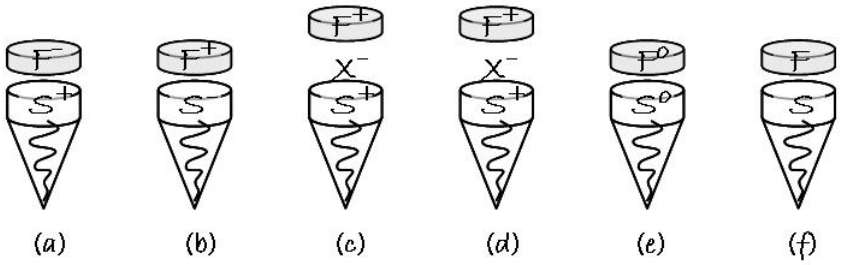

Fig. 4. Schematic representation of the various types of framework precursor–surfactant head group interactions: electrostatic S^+F^- (a), S^-F^+ (b), $S^+X^-F^+$ (c), and $S^-X^+F^-$ (d) hydrogen bonding S^0F^0 (e), and covalent bonding S–F (f).

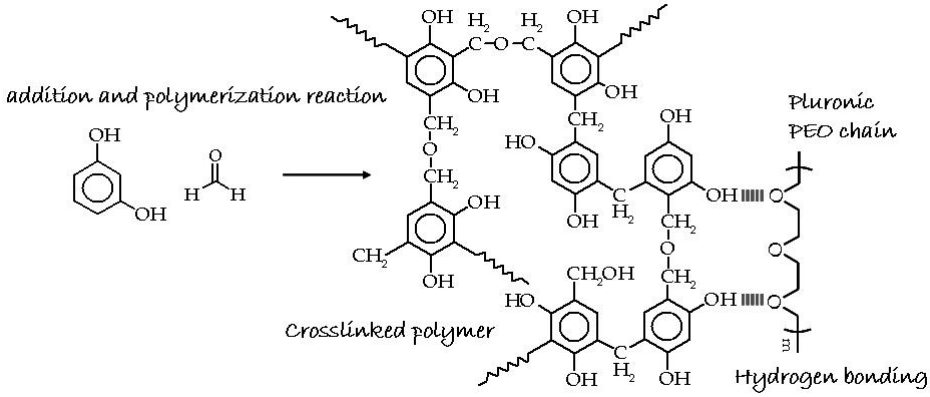

Fig. 5. Schematic representation of the reaction of resorcinol with formaldehyde and hydrogen-bonding interaction between PEO-containing block-copolymers and the hydroxyl-group-containing organic precursors.

The commercially available Pluronic block copolymers, e.g., F127, P123, and F108, have been used as templates (Fig. 3). To fabricate mesostructure, it is important to adjust the chemistry of the template head groups that can fit the requirement of the carbon precursors. The molecular interaction between the template head group and framework precursor can be expected using conventional reaction schemes. Six different possible molecular reaction pathways which use the principle of surfactant liquid crystal templating have been identified: (S^+F^-), (S^-F^+), ($S^+X^-F^+$), ($S^-X^+F^-$), (S^0F^0), and (S–F), where S is the surfactant (cationic S^+, anionic S^-, neutral S^0), F is the soluble framework precursor (cationic F^+, anionic F^-, neutral F^0), and X is the intermediated (cationic X^+, anionic X^-) molecular species (Fig. 4). S–F indicates systems where the framework specie is covalently bonded to the template. The pathway applicable to a particular synthesis will be dictated by the reagents and synthesis conditions and can be influence the physical and chemical properties of the product. Hydrogen-bonding interaction between the copolymer template and the phenolic polymer resin is an efficient route to prepare mesoporous carbons (Fig. 5).

2.1 Synthesis of ordered mesoporous carbons using organic templates

In a typical synthesis, phenolic resin monomers were completely dissolved in a mixture composed of deionized water, ethanol and hydrochloric acid. Pluronic F127 was then added, and after it was completely dissolved, formaldehyde (37 wt.%) was added to the solution. The final molar composition of the solution was 4 phenolic resin monomers : 1 : 0.005–0.05 Pluronic F127 : 9 formaldehyde : 0.1 HCl : 20–100 ethanol : 40 water. The solutions were left at room temperature, during which they separated into two phases. The transparent upper phase was ethanol–water rich and the lower dark brown phase was polymer-rich. The upper clear phase was discarded; the lower dark brown phase was preheated at 100 °C for 1 h in air. Subsequently, the resultant brown sample was carbonized under a nitrogen atmosphere at 200–800 °C.

On the basis of the thermosetting resorcinol/formaldehyde resins, ordered mesoporous carbons, designated as COU, have been synthesized via the triblock copolymer F127-

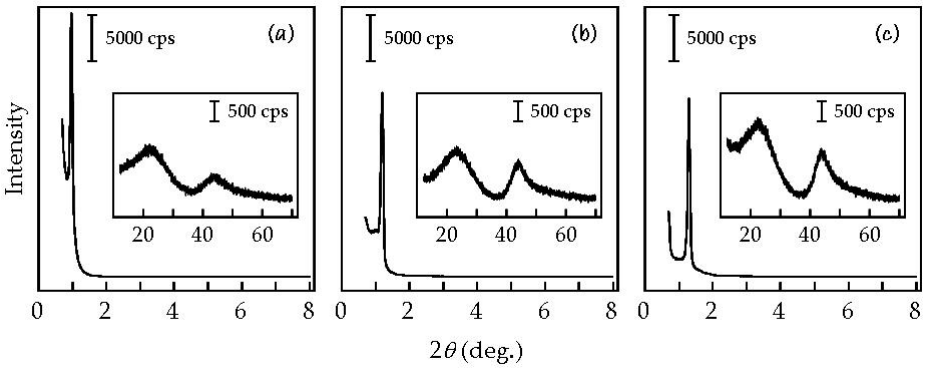

Fig. 6. XRD patterns of carbonized COU-1. The carbonization temperatures were (a) 400 °C, (b) 600 °C, and (c) 800 °C. (Tanaka et al., 2005)

templating route with the addition of triethyl orthoacetate as a co-carbon source. Fig. 6 shows X-ray diffraction (XRD) patterns of ordered mesoporous carbons COU-1. XRD pattern revealed a sharp reflection peak at a 2θ angle of 0.9–1.3°, demonstrating the periodically ordered structure of the carbons. The key to the success of their synthetic procedure was the formation of a periodically ordered organic–organic nanocomposite composed of thermosetting polymeric carbon precursors and the use of a thermally decomposable triblock copolymer Pluronic F127. Ordered mesoporous carbons COU-1 carbonized at different temperatures show typical type-IV N_2 adsorption/desorption curves with hysteresis loops, ascribed to the uniform mesopores inside the carbons (Fig. 7). The pore diameters of COU-1 carbonized at 400, 600 and 800 °C were estimated to be 7.4, 6.2 and 5.9 nm, respectively. The field-emission SEM images clearly show the hexagonally arranged channel pores and strongly support the results of the XRD and N_2 adsorption measurements (Fig. 8). Ordered straight channels have never before been seen in ordered mesoporous carbons synthesized by the inorganic-templating method.

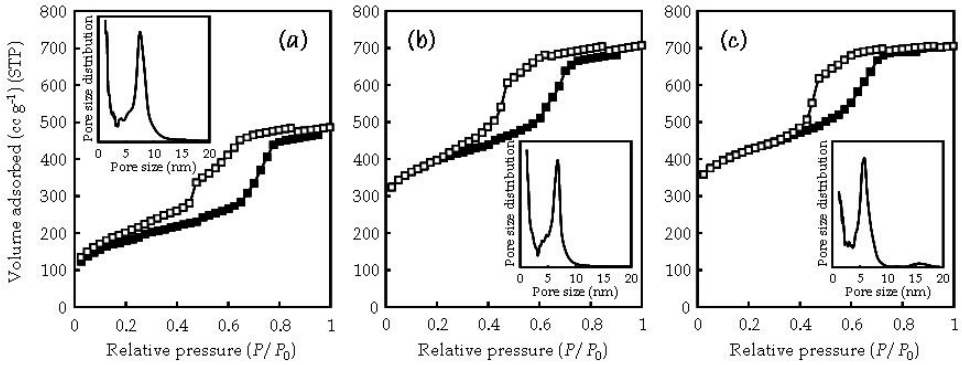

Fig. 7. N_2 adsorption/desorption isotherms and pore size distribution (inset) for carbonized COU-1. The carbonization temperatures were (a) 400 °C, (b) 600 °C, and (c) 800 °C. (Tanaka et al., 2005)

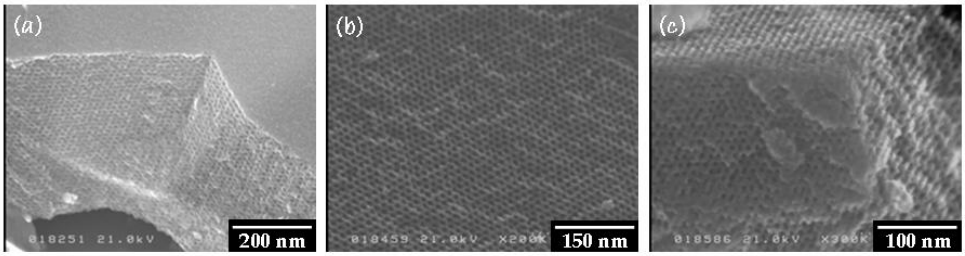

Fig. 8. FESEM images of carbonized COU-1. The carbonization temperatures were (a) 400 °C, (b) 600 °C, and (c) 800 °C. (Tanaka et al., 2005)

The surfactant F127 must have decomposed below 400 °C, because mesopores were already generated in the COU-1 carbonized at 400 °C. The thermosetting RF polymer remained as the carbonaceous pore walls, while the Pluronic F127 decomposed to form the mesopores. The increase in the micropore volume and the BET surface area at 600 °C must be due to the generation of gases from the decomposition of the RF polymer. The molar ratios of C/H were increased with increasing the carbonization temperature. The large increase in the C/H ratio at 800 °C indicates that the decomposition of the RF polymer still continued at 600–800 °C, although the micropore volume and the BET surface area showed no further increase above 600 °C.

2.2 Synthesis of hierarchically ordered mesoporous carbons

Although the inorganic-templating method is quite attractive, one should keep it in mind that this technique requires both the use of an expensive template and its removal by a severe treatment, which hampers the practical use of the template technique. On the other hand, because the template can be water-soluble in the organic-templating technique, the process would be much simpler and could be performed at low cost. Furthermore, it is noted that the organic-templating approach is advantageous for controlling the morphology and configuration and one can be use the inorganic template, which have larger template structure than that of Pluronic triblock copolymer, for preparation of mesoporous carbons with hierarchical porous structures.

The use of AAO films, which have uniform straight channels with 10–250 nm diameters, as templates for the synthesis of carbon deposits on the channel walls has been successful (Kyotani et al., 1995, 2006). The resulting tubular carbon materials have tunable diameters, lengths, and wall thickness. Additionally, the uniformity of the carbon nanostructures had never been seen before in carbon nanotubes when compared with carbon nanostructures prepared by conventional arc-evaporation or catalytic chemical vapor deposition (CVD) techniques.

On the other hand, a method to fabricate mesostructured silica within columnar pores of the AAO membranes via the surfactant-templating method has been developed (Yamaguchi et al., 2004). When ordered mesoporous silica is synthesized in film morphology, the mesostructure tends to orient with a specific (*hkl*) plane parallel to the solid–liquid interface (Hillhouse et al., 2001). When nonporous smooth substrates are used, the channel direction of the resulting mesoporous films is oriented parallel to the substrate, and transportation of molecules across the film is not possible. From the standpoint of molecular accessibility, the

channel direction of the mesoporous films should be oriented perpendicular to the film surface. Macroscopic structures of silica–surfactant mesophases grown at the interfacial region depend on the shape of the interfaces. When the silica–surfactant nanocomposite is grown inside the columnar pores, the pore wall is expected to assist the self-assembly of the silica–surfactant nanocomposite, and the resulting mesophase might be oriented along the interface.

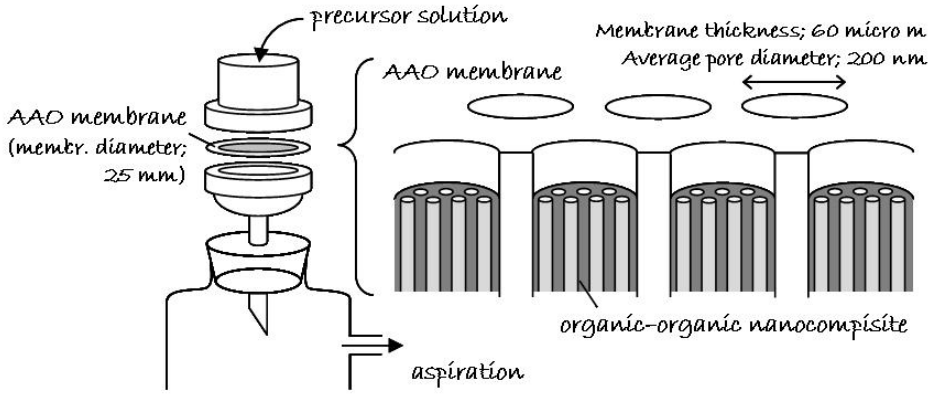

Fig. 9. Scheme to impregnate the columnar pores with triblock copolymer–templated phenolic polymer resin. Schematic illustration of the assembly of organic–organic nanocomposite formed inside the columnar alumina pores.

The procedure is quite simple and rapid; the films of triblock copolymer F127–templated phenolic polymer resin can be deposited at the columnar pore surface of the AAO membrane by simply immersing the membrane in the precursor solution. AAO membrane (average pore diameter = 200 nm, thickness = 60 μm, membrane diameter = 25 mm) was set in an ordinary membrane filtration apparatus, and the precursor solution described above was dropped onto it (Fig. 9). Moderate aspiration was applied so that the solution penetrated into the columnar alumina pores. The membrane including the precursor solution was dried in air. Carbonization was performed as described above. The AAO scaffold was completely removed by immersing the composite membrane in alkali solution.
Fig. 10 shows TEM images of mesostructured carbon nanofibers embedded within the pores of AAO membranes and released by dissolving the AAO membrane. A well-ordered structure can be obtained and the mean diameter of the mesopores in the carbon nanofibers is approximately 8 nm. The results of N_2 adsorption/desorption analysis of the mesoporous carbon nanofibers attached to the AAO membrane revealed that the pore diameter is 7.6 nm, which is in good agreement with TEM observations.
Hydrothermal stability and alkaline resistance of the nanofibers were investigated by TEM observation before and after immersing in 5 M NaOH solution at 100 °C for 24 h. For nanofibers carbonized at 400 °C, the ordered mesostructure collapses completely after alkaline hydrothermal treatment, because the framework is still composed of an intermediate between a polymer and carbon. In contrast, for nanofibers carbonized at 600 and 800 °C, the mesostructures show no difference before and after treatment. Thus,

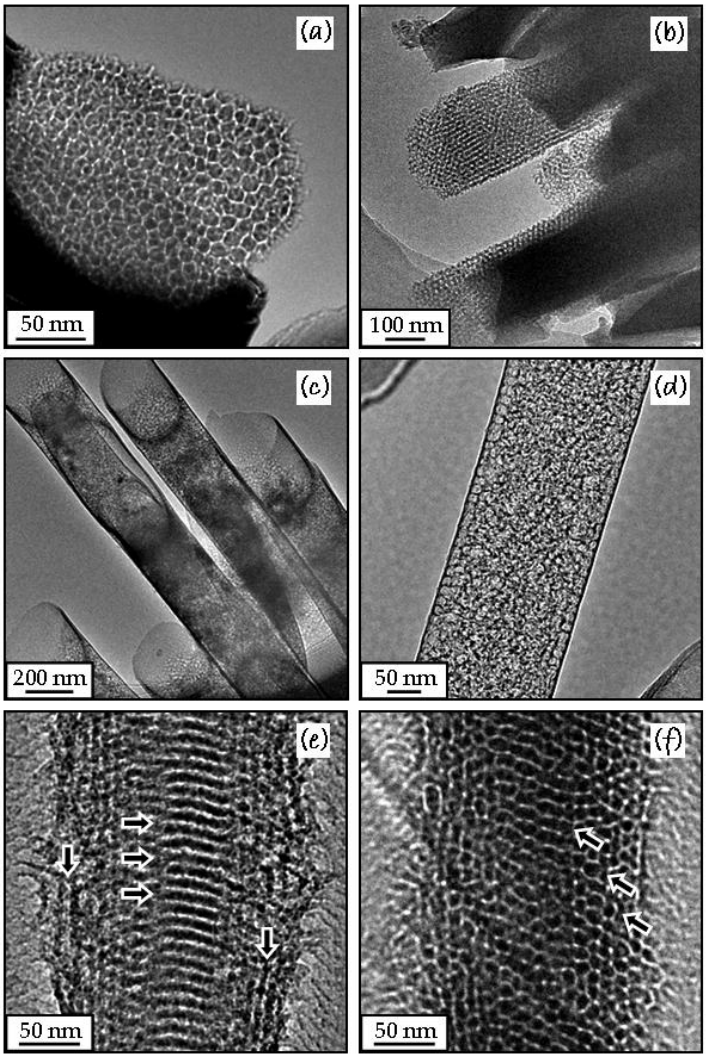

Fig. 10. (a) Top- and (b) side-view TEM images of mesoporous carbon nanofibers embedded within the pores of AAO membranes. (c) Low-magnification and (d–f) high-magnification TEM images of mesoporous carbon nanofibers after dissolving the AAO scaffolds. (Tanaka et al., 2009)

nanofibers carbonized at high temperatures (above 600 °C) show high hydrothermal stability and alkaline resistance. The longitudinal dimension and diameter of the nanofibers are about 60 μm and 200 nm, respectively, which are consistent with the pore dimension of the AAO membranes. The structural order seems to become distorted in the interior region. At the fiber–air interface, ordered layers with a short-range-order structure seem to be oriented along the interface in different directions, as indicated by the arrows.

2.3 Synthesis of ordered mesoporous carbon films and membranes

Development of well-ordered mesoporous carbon films will lead to new applications such as separation membranes and electronic devices. In the inorganic-templating method, the use of mesoporous silica thin films, rather than bulk powders, are unsuitable as a template because of the lack of pore accessibility in the silica films. Then, it is difficult to maintain the continuous film and film adhesion to the substrate may become poor.

In this section, a simple synthesis of mesoporous carbons in thin film and membrane (thick film) morphologies by means of organic–organic self-assembly using phenolic resin monomers and Pluronic F127 is introduced. Completely continuous films composed of ordered mesoporous carbon can be obtained by dip-coating or spin-coating.

Fig. 11 shows an FESEM image of a cross-section of ordered mesoporous carbon film. The color of the film turned black after carbonization at 400 °C. A continuous and flat film about 600 nm thick was grown from the silicon substrate. The carbon films were tightly adhered to the substrate even after carbonization at 800 °C. Increasing ethanol/water molar ratio and consequent decreasing concentration of the component decreases film thickness. In addition, film thickness can be controlled by adjusting the withdrawal rate during dip-coating.

When ordered mesoporous materials are synthesized in film morphology, the mesostructure tends to orient with a specific (*hkl*) plane parallel to the substrate. As such, film lattice constants are notoriously difficult to identify from XRD patterns alone, because of the limited number of observed peaks. Additionally, it was demonstrated that refraction effects of XRD are not negligible for many of the mesostructured films (Tanaka et al., 2006). To remedy this, the mesophase topology, order, and orientation of the films should be characterized by the combination of grazing-incidence small angle X-ray scattering (GISAXS), FESEM, and TEM measurements.

The molar ratio of phenolic resin monomers to F127 was changed from 115 to 800 by varying the concentration of the F127. The films prepared at phenolic resin monomers/F127 molar ratio of 200 and 160 are referred to as CKU-F69 and CKU-C12, respectively. GISAXS patterns were collected from CKU-F69 films carbonized at temperatures from 200 to 800 °C (Fig. 12). Interpretation of the GISAXS patterns was aided by NANOCELL (Tate et al., 2006), a program which simulates quantitatively the positions of Bragg diffraction peaks based on the distorted-wave Born approximation (DWBA) to account for the effects of refraction and reflection at the film–substrate and film–air interfaces. The experimental results were fitted to a face-centered orthorhombic *Fmmm* structure with the (010) planes parallel to the substrate, but where other planes were free to rotate about the substrate normal. The mesophase with cell parameters and orientation with respect to the substrate is shown schematically in Fig. 12. On the other hand, the CKU-C12 is (10)-oriented and possesses a rectangular *c*2*mm* symmetry, which results from uniaxial contraction of 2D hexagonal *p6mm* symmetry. The mesostructure were controlled by simply adjusting the molar ratio of RP/F127.

Upon the initial assembly, it is conjectured that the mesostructure is described by the body-centered lattice, likely a (110) oriented *Im*3*m* cubic close packing of micellar aggregates. The *Fmmm* mesostructure results from uniaxial shrinkage of *Im*3*m* symmetry along the substrate normal. In addition to the Bragg diffraction peaks in the GISAXS patterns, there is a diffuse ring present in the pattern. A diffraction ring superimposed on the octagon-shaped spot pattern indicates the presence of some polyoriented domains in the film. In other words some domains are not perfectly aligned about the substrate normal. Furthermore, the critical

angle for X-ray scattering from the mesoporous carbon film was measured by GISAXS. The critical angle decreased from 0.16° to 0.15° after carbonization at 400 °C, indicating the reduction of the average electron density of the film due to removal of the template. In addition, at carbonization above 600 °C further reduction of the critical angle to 0.14° indicates a decrease in the density of the carbonaceous framework.

The ordered mesostructures were also preserved during this high temperature carbonization process. However, the interplanar distance, $d010$, did decrease, and at the same time there was a decrease in the film thickness as measured by using FESEM that followed a similar trend. The shrinkage percentage of the film carbonized at 800 °C was calculated to be 68%. The majority of the decrease in the $d010$ value was observed at a carbonization temperature of 400 °C, which corresponds to 66% of total contraction. This result implies that the majority of the residual hydroxyl groups in the carbonaceous walls condense at elevated temperatures. This temperature also corresponds to the decomposition of the majority of the organic template, as described in detail below using nitrogen sorption and thermogravimetric analyses. In contrast to the changes observed in the b lattice constant, the other parameters, a and c, did not change during the carbonization process, indicating that the shrinkage in the directions parallel to the substrate was hindered by the adhesion of the coating.

The pores have an ellipsoidal shape due to anisotropic contraction upon drying and the carbonization process, in contrast to isotropic contraction for bulk powders without a support medium. Besides the uniformity of the pore size, the pore shape may be useful for limiting the sizes or orientations of guest molecules in separation, catalysis, and sensor applications. From TEM observations, it was found that many domains exist and are oriented parallel to the substrate with different rotational directions. Highly ordered patterns of cage-like pores support the conclusion that CKU-F69 products possess orthorhombic *Fmmm* symmetry.

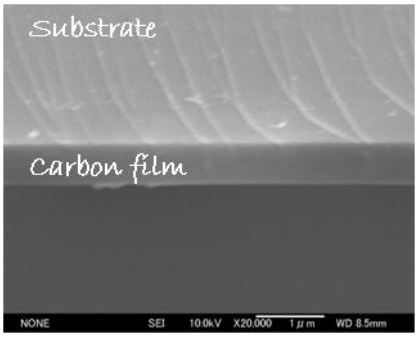

Fig. 11. FESEM image for the cross-section of CKU-F69. (Tanaka et al., 2007)

Microporous and mesoporous inorganic membranes have been investigated mainly with respect to silica membrane prepared by the sol–gel method (Park et al., 2001; Nishiyama et al., 2003; Sakamoto et al., 2007). However, silicate materials dissolved in water and alkaline solutions, which decrease the possibility of practical use. On the other hand, carbon membranes have attracted increasing interest because of their advantages, such as high surface area, high hydrothermal stability, and chemical inertness. Ordered mesoporous

carbon is a promising material in the field of membrane filtration technologies, such as nanofiltration and ultrafiltration.

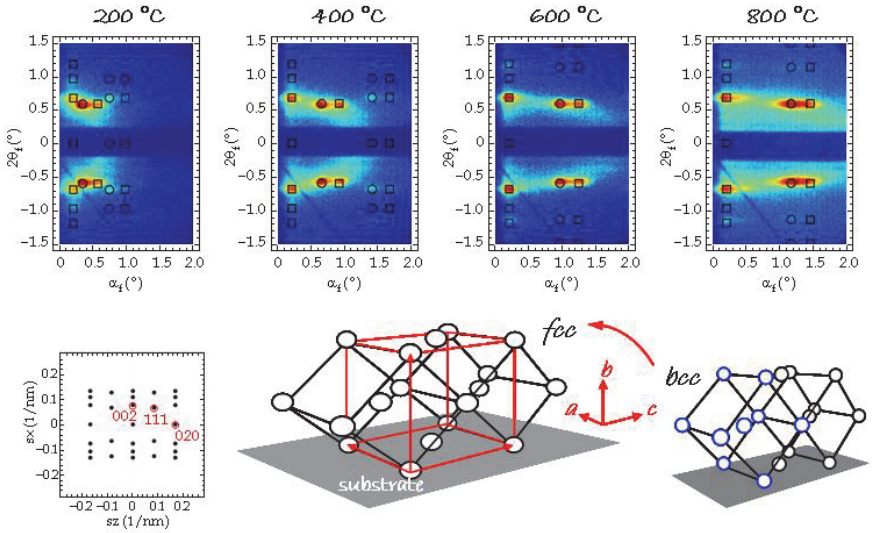

Fig. 12. GISAXS patterns of CKU-F69 carbonized at 200–800 °C. The overlay of simulated spots is from a NANOCELL simulation. The circles and squares identify transmitted and reflected Bragg peaks, respectively. In addition, NANOCELL simulated reciprocal space of an (010) oriented *Fmmm* with many domain orientations about the substrate normal. Schematic showing the cell parameters and orientation of the *Fmmm* structure with respect to the substrate. (Tanaka et al., 2007)

Next, mesoporous carbon membranes were prepared on the porous α-alumina support. α-Alumina porous tubular supports (outer diameter: 10 mm, inner diameter: 7 mm, length: 35mm, average pore size: 100 nm, average porosity: 40%) were purchased from Noritake Co., Ltd., Japan. To prepare cylindrical porous α-alumina tubes with dead-end structure, a 20 mm section of the porous α-alumina tube was joined to a dense α-alumina tube (outside diameter: 10 mm, inner diameter: 7 mm, length: 250 mm) and an α-alumina disk (diameter: 12 mm, thickness: 2 mm) with a SiO_2–BaO–CaO sealant and then calcined at 1100 °C. Membranes were prepared by dip-coating the α-alumina porous tubular support in the coating solution.

The lattice *d*-spacing of ordered mesoporous carbon membrane carbonized at 600 °C was 5.6 nm. The BET surface area and the total pore volume were 670 m^2/g and 0.58 cc/g, respectively. The pore diameter calculated from N_2 adsorption branch was estimated as 4.2 nm. The pore accessibility can be determined by the pore entrance diameter, which is useful for the limiting the sizes or orientations of guest molecules in separation, catalysis, and sensor applications.

A continuous and smooth layer about 5 μm thick was formed on the support surface. From the EDX analysis, the membrane had a carbon/alumina composite layer with a thickness of about 3.5 μm because a coating solution penetrated into the alumina pores. The ordered

mesostructures were also preserved during this high temperature carbonization process, although the carbonization of the membrane shrunk the ordered structure, which corresponds to 5% contraction. Gas permeation measurements were carried out using N_2 to confirm the compactness of the membranes. In the permeation test, a total pressure on the feed side was kept constant in the range of 75–180 kPa and the permeate side was kept constant at atmospheric pressure. The permeance of N_2 through the alumina support increased with increasing the pressure drops, suggesting that the contribution of viscous flow cannot be negligible for the alumina support. In contrast, the permeances of N_2 through the mesoporous carbon membranes were independent of the pressure drops across the membranes. The N_2 gas permeance through the mesoporous carbon membranes is predominantly governed by the Knudsen diffusion (Uhlhorn et al., 1989). These results strongly indicate that there are no important pinholes and/or defects in the membranes.
The moisture and alkaline resistance is one of the most important factors in the filed of membrane separation (Park et al., 2001; Nishiyama et al., 2003). The membranes were placed under extremely severe hydrothermal conditions (90 °C, in water) and in alkaline solution (at pH 12, for 1 week). The ordered mesostructure and gas permeation properties of the carbon membrane carbonized at 600 °C were maintained.

2.4 Control of mesostructure; effect of ethanol/water ratio

Table 1 summarizes the results of the pore structure analysis. The *d*-spacing, pore diameter, pore wall thickness, BET surface area, and pore volume change with carbonization temperature. Carbons carbonized at 400 °C have the lowest BET surface area, because the pore wall is still composed of an intermediate between a polymer and carbon. There is only a small difference in micropore volume of the samples carbonized at the same temperature but different ethanol/water molar ratios. The mesopore volume increases with increasing the ethanol/water molar ratio. Micropores are generated inside the carbonaceous framework by solidification and gasification of the polymer with a further increase in the carbonization temperature. Framework of ordered mesoporous carbon consists of imperfect graphenes of a very small size. A micropore is the space between the nanographenes. Table 1 shows that micropore volume increases with increasing pyrolysis temperature. On the other hand, the carbonization causes shrinkage of the mesostructure.
The pore size increases with increasing ethanol/water molar ratio. Control of pore size is one of the most important subjects in the study of mesoporous materials, and many methods for achieving control have been reported. The most common methods focus on the use of various swelling agents such as 1,3,5-trimethylbenzene (Beck et al., 1992), 1,3,5-triisopropylbenzene (Kimura et al., 1998), and decane (Blin et al., 2000). The strategy here is that a micellar array in which the core is composed of hydrophobic hydrocarbon chains participates in the solubilization of hydrophobic molecules. Incremental addition of the swelling agent results in an increasing pore size. This method has been shown to lead to pore expansion of up to 30%, usually accompanied by a loss of the long-range order of the mesostructure. In the organic-templating method for preparation of ordered mesoporous carbons, ethanol seems to play an important role in determining the characteristics of the porous structure. It is well known that the aqueous phase behavior of surfactants is influenced by the presence of short-chain alcohols ($n_c \geq 4$) (Ekwall et al., 1969). Unlike non-polar organics that are located at the hydrophobic core of surfactant assemblies, alcohol witha polar group (–OH group) is believed to be located at the hydrophilic–hydrophobic

EtOH/water molar ratio	T^a /°C	d^b /nm	$d_{pore\text{-}to\text{-}pore}{}^c$ /nm	D^d /nm	w^e /nm	$S_{BET}{}^f$ /m^2 g^{-1}	$V_T{}^g$ /cc g^{-1}	$V_{meso}{}^h$ /cc g^{-1}	$V_{micro}{}^i$ /cc g^{-1}
0.5	600	—	—	5.0	—	510	0.31	0.11	0.20
	800	—	—	4.0	—	490	0.24	0.04	0.20
0.75	600	—	—	5.3	—	540	0.34	0.13	0.21
	800	—	—	4.8	—	550	0.30	0.08	0.22
1.0	400	15.5	17.9	6.8	11.1	270	0.27	0.17	0.10
	600	—	—	5.8	—	530	0.40	0.19	0.21
	800	—	—	5.0	—	520	0.34	0.12	0.22
1.25	400	15.5	17.9	6.9	11.0	330	0.39	0.26	0.13
	600	—	—	6.0	—	520	0.40	0.20	0.20
	800	—	—	5.2	—	510	0.36	0.15	0.21
2.5	400	16.7	19.3	7.6	11.7	530	0.66	0.46	0.20
	600	15.5	17.9	7.2	10.7	650	0.72	0.50	0.22
	800	12.3	14.2	5.7	8.5	640	0.57	0.33	0.25

[a] Carbonization temperature. [b] *d*-spacing calculated from SAXS or Fourier diffractogram of TEM. [c] Distance between pores calculated by the formula $2d/\sqrt{3}$ assuming a hexagonal unit cell. [d] Pore diameter calculated by the BJH method using adsorption branches. [e] Pore wall thickness calculated by subtracting the pore size from the distance between pores. [f] BET surface area. [g] Total pore volume calculated as the amount of nitrogen adsorbed at a relative pressure of 0.95. [h] Mesopore volume calculated by subtracting the amount of nitrogen adsorbed at a relative pressure of 0.1 from that at a relative pressure of 0.95. [i] Micropore volume calculated from the amount of nitrogen adsorbed at a relative pressure of 0.1.

Table 1. Structure characteristics of mesoporous carbon powders prepared using different amounts of ethanol. (Tanaka et al., 2009)

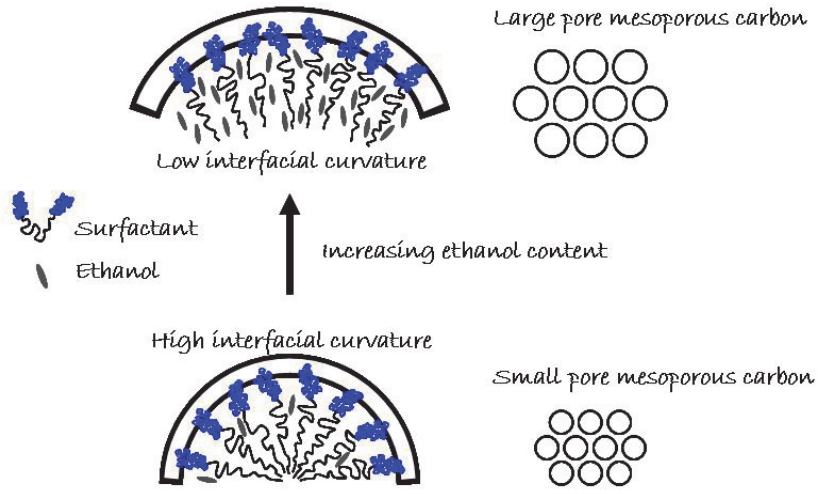

Fig. 13. Schematic representation of the role of ethanol as a swelling agent. (Tanaka et al., 2009)

interface to help stabilize liquid crystals and determine their surface curvatures. The method for controlling the mesostructure composed of silica using a ternary triblock copolymer–butanol–water system has been reported, as well as similar systems using pentanol and hexanol instead of butanol (Feng et al., 2000; Kleitz et al., 2004; Kim et al., 2005). The addition of these alcohols, which act as cosurfactants or swelling agents, results in not only increased pore size but also formation of a mesophase with a decreased curvature.
Fig. 13 shows that the mesophase may change with the micellar interfacial curvature, which varies with ethanol content. Ethanol swells the hydrophobic volume of the triblock copolymer micelles and interacts with both PPO and PEO segments because it is highly polar molecule. Thus, ethanol is located at the hydrophilic–hydrophobic interface (PEO/PPO) and stabilizes the interface, leading to the formation of micellar aggregates with decreased interfacial curvature.

3. Conclusion

As has been demonstrated in this chapter, the organic-templating approach is a very powerful method for the preparation of various types of ordered mesoporous carbons. The supramolecular templating technique opens an avenue for ordered mesoporous carbons and has advantages for controlling the morphology and configuration. The recent progress made in the development of organic-templating method was reviewed. Research efforts to produce ordered mesoporous carbons have focused on the use of phenolic polymer resins and thermally-decomposable Pluronic triblock copolymers. The choice of an appropriate set of thermosetting polymers and thermally-decomposable organic templates is the most important factor in controlling the mesophase topologies and morphology control of ordered mesostructured carbons. In powder preparation by simple precipitation process, the addition of ethanol expands both the pore size and *d*-spacing. An approach using a copolymer–alcohol–water system can be advantageous for tuning pore size even in the synthesis of mesoporous carbons. In film preparation, self-assembly of triblock copolymer–phenolic resin nanocomposites is affected by the substrate surface and mesostructure oriented parallel to the substrate. In nanofiber preparation using AAO membranes as a nanosized mold, the alumina walls may also assist the growth of the mesostructure of triblock copolymer–phenolic resin nanocomposites. The direct triblock-copolymer-templating method using an ethanol/water system provides a simple route to fabricating mesoporous carbon and carbon–polymer materials with controlled morphology. Because of their high surface area, large pore volume, and large pore size, the mesoporous carbons have potential application in capacitors, electrodes for batteries, fuel cells, chemical sensors, bioseparations, and as hosts for the immobilization of biomolecules. For many biotechnological applications, mesoporous carbons having large interconnected porous structures need to be fabricated. For the capacitors and electrodes of electrochemical devices, carbons with highly graphitic structures are needed. The synthesis and application of hierarchical porous carbons are expected in the future. These future works have been very challenging. Simple template synthetic procedures will expand the possibility of synthesizing a variety of ordered porous carbon and carbon–polymer materials.

4. Acknowledgment

This work was supported by the Kinki Invention Center, the Murata Science Foundation (A91153), and the Japan Society for the Promotion of Science (JSPS) (KAKENHI #19860074

and #21760562). The GISAXS patterns were collected at the NSF funded facility for In-situ X-ray Scattering from Nanomaterials and Catalysts (MRI program award 0321118-CTS). The authors thank Dr. M. P. Tate and Associate Prof. H. W. Hillhouse (Purdue University) for the GISAXS measurements.

5. References

Kroto, H. W.; Heath, J. R.; O'Brien, S. C.; Curl, R. F. & Smalley, R. E. (1985). C-60 – buckminsterfullerene, *Nature*, Vol. 318, No. 6042, pp. 162–163, ISSN 0028–0836

Iijima, S. (1991). Helical microtubules of graphitic carbon, *Nature*, Vol. 354, No. 6348, pp. 56–58, ISSN 0028–0836

Marsh, H. & Rand, B. (1971). The process of activation of carbons by gasification with CO_2-II. The role of catalytic impurities, *Carbon*, Vol. 9, No. 1, pp. 63–72, ISSN 0008–6223

Tamai, H.; Kakii, T.; Hirota, Y.; Kumamoto, T. & Yasuda, H. (1996). Synthesis of extremely large mesoporous activated carbon and its unique adsorption for giant molecules, *Chem. Mater.*, Vol. 8, No. 2, pp. 454–462, ISSN 0897–4756

Hu, Z.; Srinivasan, M. P. & Ni, Y. (2000). Preparation of mesoporous high-surface-area activated carbon, *Adv. Mater.*, Vol. 12, No. 1, pp. 62–65, ISSN 0935–9648

Kyotani, T.; Tsai, L. –F. & Tomita, A. (1995). Formation of ultrafine carbon tubes by using an anodic aluminum-oxide film as a template, *Chem. Mater.*, Vol. 7, No. 8, pp. 1427–1428, ISSN 0897–4756

Kyotani, T. (2006). Synthesis of various types of nano carbons using the template technique, *Bull. Chem. Soc. Jpn.*, Vol. 79, No. 9, pp. 1322–1337, ISSN 0009–2673

Kyotani, T.; Nagai, T.; Inoue, S. & Tomita, A. (1997). Formation of new type of porous carbon by carbonization in zeolite nanochannels, *Chem. Mater.*, Vol. 9, No. 2, pp. 609–615, ISSN 0897–4756

Ma, Z.; Kyotani, T. & Tomita, A. (2000). Preparation of a high surface area microporous carbon having the structural regularity of Y zeolite, *Chem. Commun.*, No. 23, pp. 2365–2366, ISSN 1359–7345

Nishihara, H; Yang, Q. –H.; Hou, P. –X.; Unno, M.; Yamauchi, S.; Saito, R.; Paredes, J. I.; Martinez-Alonso, A.; Tascon, J. M. D.; Sato, Y.; Terauchi, M. & Kyotani, T. (2009). A possible buckybowl-like structure of zeolite templated carbon, *Carbon*, Vol. 47, No. 5, pp. 1220–1230, ISSN 0008–6223

Zakhidov, A. A.; Baughman, R. H.; Iqbal, Z.; Cui, C.; Khayrullin, I.; Dantas, S. O.; Marti, J. & Ralchenko, V. G. (1998). Carbon structures with three-dimensional periodicity at optical wavelengths, *Science*, Vol. 282, No. 5390, pp. 897–901, ISSN 0036–8075

Yu, J. –S.; Kang, S.; Yoon, S. B. & Chai, G. (2002). Fabrication of ordered uniform porous carbon networks and their application to a catalyst supporter, *J. Am. Chem. Soc.*, Vol. 124, No. 32, pp. 9382–9383, ISSN 0002–7863

Ryoo, R.; Joo, S. H. & Jun, S. (1999). Synthesis of highly ordered carbon molecular sieves via template-mediated structural transformation, *J. Phys. Chem. B*, Vol. 103, No. 37, pp. 7743–7746, ISSN 1089–5647

Lee, J.; Yoon, S.; Hyeon, T.; Oh, S. M. & Kim, K. B. (1999). Synthesis of a new mesoporous carbon and its application to electrochemical double-layer capacitors, *Chem. Commun.*, No. 21, pp. 2177–2178, ISSN 1359–7345

Kaneda, M.; Tsubakiyama, T.; Carlsson, A.; Sakamoto, Y.; Ohsuna, T.; Terasaki, O.; Joo, S. H. & Ryoo, R. (2002). Structural study of mesoporous MCM-48 and carbon networks synthesized in the spaces of MCM-48 by electron crystallography, *J. Phys. Chem. B*, Vol. 106, No. 6, pp. 1256–1266, ISSN 1520–6106

Kleitz, F.; Choi, S. H. & Ryoo, R. (2003). Cubic *Ia3d* large mesoporous silica: synthesis and replication to platinum nanowires, carbon nanorods and carbon nanotubes, *Chem. Commun.*, No. 17, pp. 2136–2137, ISSN 1359–7345

Xia, Y.; Yang, Z. & Mokaya, R. (2006). Simultaneous control of morphology and porosity in nanoporous carbon: Graphitic mesoporous carbon nanorods and nanotubules with tunable pore size, *Chem. Mater.*, Vol. 18, No. 1, pp. 140–148, ISSN 0897–4756

Kresge, C. T.; Leonowicz, M. E.; Roth, W. J.; Vartuli, J. C. & Beck, J. S. (1992). Ordered mesoporous molecular-sieves synthesized by a liquid-crystal template mechanism, *Nature*, Vol. 359, No. 6397, pp. 710–712, ISSN 0028–0836

Beck, J. S.; Vartuli, J. C.; Roth, W. J.; Leonowicz, M. E.; Kresge, C. T.; Schmitt, K. D.; Chu, C. T. W.; Olson, D. H.; Sheppard, E. W.; McCullen, S. B.; Higgins, J. B. & Schlenker, J. L. (1992). A new family of mesoporous molecular-sieves prepared with liquid-crystal templates, *J. Am. Chem. Soc.*, Vol. 114, No. 27, pp. 10834–10843, ISSN 0002–7863

Zhao, D.; Huo, Q.; Feng, J.; Chmelka, B. F. & Stucky, G. D. (1998). Nonionic triblock and star diblock copolymer and oligomeric surfactant syntheses of highly ordered, hydrothermally stable, mesoporous silica structures, *J. Am. Chem. Soc.*, Vol. 120, No. 24, pp. 6024–6036, ISSN 0002–7863

Tanaka, S.; Nishiyama, N.; Egashira, Y. & Ueyama, K. (2005). Synthesis of ordered mesoporous carbons with channel structure from an organic-organic nanocomposite, *Chem. Commun.*, No. 16, pp. 2125–2127, ISSN 1359–7345

Tanaka, S.; Katayama, Y.; Tate, M. P.; Hillhouse, H. W. & Miyake, Y. (2007). Fabrication of continuous mesoporous carbon films with face-centered orthorhombic symmetry through a soft templating pathway, *J. Mater. Chem.*, Vol. 17, No. 34, pp. 3639–3645, ISSN 0959–9428

Tanaka, S.; Doi, A.; Nakatani, N.; Katayama, Y. & Miyake, Y. (2009). Synthesis of ordered mesoporous carbon films, powders, and fibers by direct triblock-copolymer-templating method using an ethanol/water system, *Carbon*, Vol. 47, No. 11, pp. 2688–2698, ISSN 0008–6223

Jin, J.; Tanaka, S.; Egashira, Y. & Nishiyam, N. (2010). KOH activation of ordered mesoporous carbons prepared by a soft-templating method and their enhanced electrochemical properties, *Carbon*, Vol. 48, No. 7, pp. 1985–1989, ISSN 0008–6223

Jin, J.; Nishiyama, N.; Egashira, Y. & Ueyama, K. (2009). Pore structure and pore size controls of ordered mesoporous carbons prepared from resorcinol/formaldehyde/ triblock polymers, *Micropor. Mesopor. Mater.*, Vol. 118, No. 1–3, pp. 218–223, ISSN 1387–1811

Simanjuntak, F. H.; Jin, J.; Nishiyama, N.; Egashira, Y. & Ueyama, K. (2009). Ordered mesoporous carbon films prepared from 1,5-dihydroxynaphthalene/triblock copolymer composites, *Carbon*, Vol. 47, No. 10, pp. 2531–2533, ISSN 0008–6223

Meng, Y.; Gu, D.; Zhang, F. Q.; Shi, Y. F.; Yang, H. F.; Li, Z.; Yu, C.; Tu, B. & Zhao, D. (2005). Ordered mesoporous polymers and homologous carbon frameworks: Amphiphilic

surfactant templating and direct transformation, *Angew. Chem., Int. Ed.*, Vol. 44, No. 43, pp. 7053–7059, ISSN 1433–7851

Zhang, F. Q.; Meng, Y.; Gu, D.; Yan, Y.; Yu, C. Z.; Tu, B. & Zhao, D. (2005). A facile aqueous route to synthesize highly ordered mesoporous polymers and carbon frameworks with *Ia3d* bicontinuous cubic structure, *J. Am. Chem. Soc.*, Vol. 127, No. 39, pp. 13508–13509, ISSN 0002–7863

Zhang, F. Q.; Meng, Y.; Gu, D.; Yan, Y.; Chen, Z. X.; Tu, B. & Zhao, D. (2006). An aqueous cooperative assembly route to synthesize ordered mesoporous carbons with controlled structures and morphology, *Chem. Mater.*, Vol. 18, No. 22, pp. 5279–5288, ISSN 0897–4756

Pekala, R. W. (1989). Organic aerogels from the polycondensation of resorcinol with formaldehyde, *J. Mater. Sci.*, Vol. 24, No. 9, pp. 3221–3227, ISSN 0022–2461

Yamaguchi, A.; Uejo, F.; Yoda, T.; Uchida, T.; Tanamura, Y.; Yamashita, T. & Teramae, N. (2004). Self-assembly of a silica-surfactant nanocomposite in a porous alumina membrane, *Nature Mater.*, Vol. 3, No. 5, pp. 337–341, ISSN 1476–1122

Hillhouse, H. W.; Egmond, J. W.; Tsapatsis, M.; Hanson, J. C. & Larese, J. Z. (2001). The interpretation of X-ray diffraction data for the determination of channel orientation in mesoporous films, *Micropor. Mesopor. Mater.*, Vol. 44–45, pp. 639–643, ISSN 1387–1811

Tanaka, S.; Tate, M. P.; Nishiyama, N.; Ueyama, K. & Hillhouse, H. W. (2006). Structure of mesoporous silica thin films prepared by contacting PEO_{106}-PPO_{70}-PEO_{106} films with vaporized TEOS, *Chem. Mater.*, Vol. 18, No. 23, pp. 5461–5466, ISSN 0897–4756

Tate, M. P.; Urade, V. N.; Kowalski, J. D.; Wei, T. C.; Hamilton, B. D.; Eggiman, B. W. & Hillhouse, H. W. (2006). Simulation and interpretation of 2D diffraction patterns from self-assembled nanostructured films at arbitrary angles of incidence: From grazing incidence (above the critical angle) to transmission perpendicular to the substrate, *J. Phys. Chem. B*, Vol. 110, No. 20, pp. 9882–9892, ISSN 1520–6106

Park, D. H.; Nishiyama, N.; Egashira, Y. & Ueyama, K. (2001). Enhancement of hydrothermal stability and hydrophobicity of a silica MCM-48 membrane by silylation, *Ind. Eng. Chem. Res.*, Vol. 40, No. 26, pp. 6105–6110, ISSN 0888–5885

Nishiyama, N.; Saputra, H.; Park, D. H.; Egashira, Y. & Ueyama, K. (2003). Zirconium-containing mesoporous silica Zr-MCM-48 for alkali resistant filtration membranes, *J. Membr. Sci.*, Vol. 218, No. 1–2, pp. 165–171, ISSN 0376–7388

Sakamoto, Y.; Nagata, K.; Yogo, K. & Yamada, K. (2007). Preparation and CO_2 separation properties of amine-modified mesoporous silica membranes, *Micropor. Mesopor. Mater.*, Vol. 101, No. 1–2, pp. 303–311, ISSN 1387–1811

Uhlhorn, R. J. R.; Keizer, K. & Burggraaf, A. J. (1989). Gas and surface-diffusion in modified gamma-alumina systems, *J. Membr. Sci.*, Vol. 46, No. 23, pp. 225–241, ISSN 0376–7388

Kimura, T.; Sugahara, Y. & Kuroda, K. (1998). Synthesis of mesoporous aluminophosphates using surfactants with long alkyl chain lengths and triisopropylbenzene as a solubilizing agent, *Chem. Commun.*, No. 5, pp. 559–560, ISSN 1359–7345

Blin, J. L. ; Otjacques, C.; Herrier, G. & Su, B. L. (2000). Pore size engineering of mesoporous silicas using decane as expander, *Langmuir*, Vol. 16, No. 9, pp. 4229–4236, ISSN 0743–7463

Ekwall, P.; Mandell, L. & Fontell, K. (1969). The cetyltrimethylammonium bromide-hexanol-water system, *J. Colloid. Interf. Sci.*, Vol. 29, No. 4, pp. 639–646, ISSN 0021–9797

Feng, P. Y.; Bu, X. H. & Pine, D. J. (2000). Control of pore sizes in mesoporous silica templated by liquid crystals in block copolymer-cosurfactant-water systems, *Langmuir*, Vol. 16, No. 12, pp. 5304–5310, ISSN 0743–7463

Kleitz, F.; Solvyov, L. A.; Anilkumar, G. M.; Choi, S. H. & Ryoo, R. (2004). Transformation of highly ordered large pore silica mesophases (*Fm*3*m*, *Im*3*m* and *p*6*mm*) in a ternary triblock copolymer-butanol-water system, *Chem. Commun.*, No. 13, pp. 1536–1537, ISSN 1359–7345

Kim, T. W.; Kleitz, F.; Paul, B. & Ryoo, R. (2005). MCM-48-like large mesoporous silicas with tailored pore structure: Facile synthesis domain in a ternary triblock copolymer-butanol-water system, *J. Am. Chem. Soc.*, Vol. 127, No. 20, pp. 7601–7610, ISSN 0002–7863